# Bacteria-derived peptidoglycan triggers a non-canonical NF-$\kappa$B dependent response in Drosophila gustatory neurons

Ambra Masuzzo, Gérard Manière, Yael Grosjean, Léopold Kurz, Julien Royet

# Bacteria-derived peptidoglycan triggers a non-canonical NF-κB dependent response in *Drosophila* gustatory neurons

Ambra Masuzzo[1 $], Gérard Manière[2 $], Yaël Grosjean[2 *], Léopold Kurz[1 *], Julien Royet[1 *]

1 : Aix-Marseille Université, CNRS, IBDM, Marseille, France

2 : Centre des Sciences du Goût et de l'Alimentation, L'Institut agro Dijon, CNRS, INRAE, Université Bourgogne Franche-Comté, F-21000 Dijon, France

[$] co-first author, [*] co-corresponding authors

Abbreviated title: Bacteria-derived peptidoglycan sensing by gustatory neurons

**Abstract**

Probing the external world is essential for eukaryotes to distinguish beneficial from pathogenic microorganisms. If it is clear that the main part of this task falls to the immune cells, recent work shows that neurons can also detect microbes, although the molecules and mechanisms involved are less characterized. In *Drosophila,* detection of bacteria-derived peptidoglycan by pattern recognition receptors of the PGRP family expressed in immune cells, triggers NF-κB/IMD dependent signaling. We show here that one PGRP protein, called PGRP-LB, is expressed in some proboscis's bitter gustatory neurons. *In vivo* calcium imaging in female flies reveals that the PGRP/IMD pathway is cell-autonomously required in these neurons to transduce the peptidoglycan signal. We finally show that NF-κB/IMD pathway activation in bitter-sensing gustatory neurons influences fly behavior. This demonstrates that a major immune response elicitor and signaling module are required in the peripheral nervous system to sense the presence of bacteria in the environment.

**Significance**

In addition to the classical immune response, eukaryotes rely on neuronally-controlled mechanisms to detect microbes and engage in adapted behaviors. However, the mechanisms of microbe detection by the nervous system are poorly understood. Using genetic analysis and calcium imaging, we demonstrate here that bacteria-derived peptidoglycan can activate bitter gustatory neurons. We further show that this response is mediated by the PGRP-LC membrane receptor and downstream components of a non-canonical NF-κB signaling cascade. Activation of this signaling cascade triggers behavior changes. These data demonstrate that bitter-sensing neurons and immune cells share a common detection and signaling module to either trigger the production of antibacterial effectors or to modulate the behavior of flies that are in contact with bacteria. Since PGN detection doesn't mobilize the known gustatory receptors, it also demonstrates that taste perception is much more complex than anticipated

## Introduction

Since microorganisms can reduce the fitness of their hosts, natural selection has favored defense mechanisms that protect them against disease-causing agents. The molecular mechanisms that are activated during the humoral and cellular responses, the main armed branches of the host against invading microbes, are known in great detail. By avoiding pathogenic microorganisms or modifying its behavior when infected, host can prevent the activation of the costly immune response, maximizes its efficiency and reduce the consequences of the infection on themselves or their progeny. Phenotypes related to such behaviors are well known in mammals. They range from disgust to social isolation including sleepiness [1]. These responses to the microbial environment are accepted as symptoms, but are not well defined molecularly. Observations in invertebrates phenocopying the mammalian sickness behaviors have also been made [2] and may often be interpreted in an anthropomorphic way while there is no molecular deciphering or no ecological context. For instance, social insects, such as termites can ascertain the virulence of the *Metarhizium* and *Beauveria* fungi and avoid the most virulent strains[3], while *Apis mellifera* workers are able to detect larvae infected with the fungus *Ascosphaera apis* and remove them from the nest[4]. On the other hand, since some microorganisms are beneficial for their host, animals can also be attracted by them. Up to date, the molecular and neuronal basis of these behavioral responses to microbes are much less characterized than the "canonical" immune responses. Genetically tractable models such as *Caenorhabditis elegans* or *Drosophila melanogaster* are very well suited to elucidate them [5, 6, 7, 8].

Devoid of adaptative immunity like all invertebrates, *Drosophila* has emerged as a well-adapted model to unravel the signaling modules that control the innate immune responses against bacteria [9, 10, 11, 12]. Essential to them are two NF-κB signaling pathways called Toll and IMmune Deficiency (IMD) whose activation triggers the production of immune effectors, such as AntiMicrobial Peptides (AMPs), in immune-competent cells [9, 13, 14, 15]. This activation depends on the previous detection of bacteria-derived PeptidoGlycaN (PGN) by host Pattern Recognition Receptors (PRRs) belonging to the PeptidoGlycan Recognition Protein (PGRP) family [16, 17]. Recent work has shown that signaling components of the NF-κB/IMD pathway, including the NF-κB transcription factor Relish, and the upstream PGRP sensors are functionally required outside the immune system and more specifically in some neurons of the Central Nervous System (CNS) [18, 19]. Direct recognition of circulating bacteria-derived PGN by few brain octopaminergic neurons leads to their inhibition and, in turn, to an egg-laying reduction

in PGN-exposed females [20] [19]. Hence, by detecting a ubiquitous bacteria cell wall component via dedicated PRRs, few brain neurons adapt the female physiology to its infectious status.

The Peripheral Nervous System (PNS) of *Drosophila* and more specifically its gustatory and olfactory systems are also involved in microbe-induced behaviors. By activating a subclass of olfactory neurons that express the olfactory receptor Or56a, the microbial odorant geosmin induces pathogen avoidance by inhibiting oviposition, chemotaxis, and feeding [21]. In contrast, bacterial volatiles commonly produced during decomposition of plant material such as ammonia and certain amines, are highly attractive to flies [22]. Furthermore, Or30a-dependent detection of bacteria-derived short-chain fatty acid induces attraction in larvae[23]. Previous works demonstrated that bacterial cell wall components like LipoPolySaccharide (LPS) and PGN are detected by *Drosophila's* gustatory sensory system [24]. Detection of LPS by the esophageal bitter Gustatory Receptor Neurons (GRNs) expressing the chemosensory cation channel TrpA1 (Transient receptor potential cation channel subfamily A member 1) triggers feeding and oviposition avoidance [25]. PGN detection, instead, triggers grooming behavior upon stimulation of wing margins and legs but the nature of gustatory sensory neurons and receptors involved in this behavior remain elusive [24].

Previous work has shown that recognition of bacteria-derived PGN by fly PGRPs mediates many of these procaryotes-eucaryotes interactions. Di-Amino Pimelic PGN (DAP-type PGN) found in the cell wall of most Gram-negative bacteria is detected either at the membrane of immune competent cells by PGRP-LC, or in the cytosol by the soluble PGRP-LE receptor [26, 27, 28]. In both cases, this recognition step is sufficient to activate the evolutionary conserved NF-κB downstream signaling cascade that, in turn, will induce the production of antibacterial molecules. Probably because its prolonged activation is detrimental for the host, NF-κB pathway activation levels are finely modulated by several negative regulators [29]. Among them are enzymes, called amidases, that by binding and cleaving the PGN into inactive products buffer IMD pathway activation. PGRP-LB is such an enzyme that is present either extracellularly via its PGRP-LB$^{RC}$ isoform or inside the cell via the PGRP-LB$^{RA}$ and $^{RD}$ isoforms[30, 31, 32, 33]. We present here data demonstrating that the PGRP-LB enzyme and other IMD pathway components are expressed in some gustatory neurons suggesting that these cells might sense and react to external PGN. Using genetic analysis and calcium imaging, we demonstrate that some members of the IMD pathway are functionally required in bitter-sensing gustatory neurons to sense and transduce the presence of PGN without the mobilization of the classical gustatory receptors expressed in these cells. These results demonstrate that the taste system can be used by the fly to detect the presence of PGN in the environment and that the PGRP/IMD module is not only

required in immune cells to trigger the production of antibacterial effectors but also in sensory neurons to modulate fly behavior upon bacteria sensing. Thus, the PGN that is used as an alarm signal when detected within the body cavity is as well a qualitative readout about the fly environment.

## Results

### A peptidoglycan binding protein is expressed in some bitter gustatory neurons

Our previous work has shown that some PGN sensing molecules (PGRPs) are active outside immune cells and specifically in neurons of the CNS. Indeed, the direct detection of bacteria-derived PGN by the cytosolic protein PGRP-LE in a subset of brain octopaminergic neurons modulates oviposition of infected females in an NF-κB-dependent manner [18, 20]. To identify neurons which potentially expressed PGRPs and thus respond to PGN, we previously made use of a reporter line, pLB1$^{Gal4}$, that partially recapitulates the endogenous expression of one PGRP-LB protein isoform (i.e., PGRP-LB$^{RD}$)[20] (Extended Data Fig.1-1a). We now noticed that, in addition to being expressed in some neurons of the brain, this line also labeled axonal projections that originated from neurons of the PNS. In pLB1$^{Gal4}$/UAS-mCD8-GFP flies, a GFP signal was observed in the Sub-Esophageal Zone (SEZ) of the central brain where GRNs send their axonal projections (Fig. 1a, b) [34, 35]. Accordingly, some spare cell bodies present in the labella at the position of taste sensory neurons were detected (here called pLB1+ neurons; Fig. 1c, Extended data Fig. 1-1b and Table 1). In contrast, no signal was detected using the two other PGRP-LB isoform reporter constructs pLB2$^{Gal4}$ and pLB3 $^{Gal4}$ (Extended Data Fig.1-1a, b)[18]. The axonal network within the SEZ of pLB1$^{Gal4}$/UAS-mCD8-GFP flies is reminiscent of taste neurons associated with detection of molecules triggering aversion and classified as bitter. Double staining between pLB1$^{Gal4}$/UAS-mCD8-GFP and Gr66a-RFP, which is specifically expressed in bitter gustatory neurons, revealed that all pLB1+ neurons are bitter (Gr66a+), although they only represent a sub-population of them (Fig. 1d, e and Table 2). Indeed, while there are around 25 Gr66a+ neurons per each labellum, we identified an average of 5 ± 2 pLB1+ neurons [36, 37, 38] (Table 1 and Table 2). We confirmed this result by using genetic intersectional strategy between pLB1$^{Gal4}$ and Gr66a$^{LexA}$ (Extended Data Fig. 1-2a) and by using another driver that broadly targets bitter-sensing gustatory neurons (i.e., Gr32a$^{LexA}$) (Extended Data Fig. 1-2c). Consistently, by using the same strategy and a driver that labels sweet GRNs (Gr5a$^{LexA}$), we did not detect any neurons that are simultaneously pLB1+ and Gr5a+ (Extended Data Fig. 1-2d). In addition, the expression of the Gal4 inhibitor Gal80 in Gr66a+ neurons

(Gr66a$^{LexA}$/LexAop$^{Gal80}$) suppressed the expression of GFP in pLB1+ neurons (pLB1$^{Gal4}$/UAS-mCD8-GFP). No signal was detected in pLB1$^{Gal4}$/ UAS-mCD8-GFP flies expressing the Gal80 repressor, (Extended Data Fig. 1-2b). Lastly, imaging using a pan-isoform reporter line in which the endogenous PGRP-LB has been GFP-tagged at the locus (PGRP-LB::GFP) demonstrated that the endogenous PGRP-LB protein is also produced in Gr66a+ neurons (Extended Data Fig. 1-2e). Taken together, these data demonstrate that all the pLB1+ neurons in the proboscis are bitter-sensing neurons.

**Bitter GRNs respond to bacteria and to DAP-type PGN**

Since we observed in bitter-sensing gustatory neurons the expression of an enzyme dedicated to the buffering of the NF-κB/IMD response and that the PGN is a proxy to delineate whether bacteria are present or not, we first tested whether pLB1+ gustatory neurons could be activated by bacterial PGN by performing *in vivo* calcium imaging.

Two types of PGN, which differs for a single amino acid in the stem peptide, are found in bacteria. Whereas the Lysine (Lys)-type PGN is found in Gram-positive bacteria cell wall, the DAP-type PGN forms that of Gram-negative bacteria. While Lys-type PGN preferentially triggers the *Drosophila* NF-κB/Toll pathway, DAP-type PGN mainly leads to the activation of the NF-κB/IMD pathway [26]. Exposing the labella of pLB1$^{Gal4}$/UAS-GCaMP6s flies to DAP-type PGN triggered an increase of the intracellular calcium levels in the SEZ located axonal projections of labellar pLB1+ neurons, indicating that this subset of gustatory neurons senses and is activated by bacterial DAP-type PGN. Our data demonstrated that pLB1+ neurons responded to DAP-type PGN in a dose-dependent manner and detected caffeine (a bitter compound for flies), but not sucrose, confirming their bitter nature (Fig. 2a, b, Movie 1, 2).

Considering that the pLB1$^{Gal4}$ transgene drives the expression of Gal4 in neurons other than GRNs and in immune cells, and that all pLB1+ GRNs are GR66a+, we decided to study PGN perception by bitter gustatory neurons in the well-characterized Gr66a+ GRN population. As for labellar pLB1+ gustatory neurons, calcium imaging revealed that DAP-type PGN activates Gr66a+ neurons (Fig. 2c, d, Movie 3). Together, these results showed that bitter GRNs, among which some express the PGRP-LB protein, are able to respond to DAP-type PGN. Moreover, when we exposed flies to *E. coli,* a Gram-negative bacterium that produces DAP-type PGN and known to activate the NF-κB/IMD cascade in immune tissues, we also detected a response in Gr66a+ neurons, demonstrating that these neurons are able to directly detect bacteria (Fig. 2c, d). Because of the highly complex biochemical composition of bacteria, we decided for the next

experiments to focus on the sensing of pure PGN. To evaluate the specificity of this response, pLB1$^{Gal4}$/UAS-GCaMP6s and Gr66a$^{Gal4}$/UAS-GCaMP6s flies were exposed to Lys-type PGN, that does not interact with PGRP-LB and does not activate the NF-κB/IMD cascade [26]. When used at concentrations at which DAP-type PGN is active, Lys-type PGN was unable to trigger calcium increase in pLB1+, nor in GR66a+ neurons (Fig. 2e, f). These data indicate that bitter-sensing gustatory neurons are responsive to the DAP-type PGN found in the cell wall of Gram-negative bacteria.

**Upstream elements of the NF-κB/IMD pathway are required for the response of bitter GRNs to PGN**

Since some GRNs respond to DAP-type PGN, we tested whether the canonical upstream PGN sensors and downstream NF-κB/IMD pathway components were necessary to transduce its signal, as it is for immune competent cells. For that purpose, *in vivo* calcium imaging experiments in pLB1$^{Gal4}$/UAS-GCaMP6s flies were performed in various NF-κB/IMD mutant background flies. Two PGRP proteins function as upstream DAP-type PGN (hereafter simply PGN) receptors: PGRP-LC and PGRP-LE (Fig. 3a). While caffeine response was unaffected in *PGRP-LC* (*PGRP-LC$^{E12}$*) and *PGRP-LE* (*PGRP-LE$^{112}$*) mutants (Extended Data Fig. 3-1a), PGN ability to activate pLB1+ neurons was completely abrogated in *PGRP-LC* mutants (Fig. 3b) and to a lesser extent, decreased in *PGRP-LE* animals. In contrast, PGN sensing in pLB1+ neurons was not modified in the *PGRP-LB* mutant background compared to control animals (Fig. 3b). When we studied the PGN response in Gr66a$^{Gal4}$/UAS-GCamP6s flies, the loss of PGRP-LC was also sufficient to abolish this response, indicating that this membrane-associated receptor is required in bitter-sensing neurons to detect the PGN (Fig. 3c).

Since previous reports demonstrated that elements of the NF-κB/IMD pathway are expressed and functionally required in some neurons[18, 20], their implication in mediating the effect of PGN was tested. While loss-of-function mutants for *Dredd* (*Dredd$^{D55}$*) (Fig. 3a) were responding normally to caffeine, a strong reduction of calcium signal in pLB1+ neurons was observed in flies stimulated with PGN (Fig. 3 b, c and Extended Data Fig. 3-1a, c). The conserved ability of *Dredd* mutants to detect caffeine demonstrated that their unresponsiveness to PGN was neither secondary to neuronal death nor to a loss of cell functionality. To ensure that the NF-κB/IMD pathway was required cell-autonomously in gustatory neurons, we used RNAi-mediated cell-specific inactivation. Functional downregulation of the *PGRP-LC*, *IMD*, *Fadd*, and *Dredd* in GR66a+ cells, was sufficient to block calcium response after PGN stimulation (Fig.

3d). These neurons remained responsive to caffeine (Extended Data Fig. 3-1d) demonstrating that the NF-κB/IMD pathway upstream components inactivation specifically impaired the response to PGN. Since most of the reported IMD-dependent responses have been shown to be mediated by the NF-κB transcription factor Relish, we tested its implication in bitter GRNs response to PGN [9, 13]. Intriguingly, the calcium response of Gr66a+ neurons upon proboscis stimulation by PGN or caffeine was not statistically different in *Relish* RNAi flies compared to wild-type controls (Fig. 3d and Extended Data Fig. 3-1d). Altogether, these data demonstrate that Gr66a+ neurons can respond to DAP-type PGN in an IMD-pathway dependent manner, but suggest that it is independent of the canonical Relish trans-activator.

**The response of bitter-sensing neurons to peptidoglycan does not require TrpA1 nor Gr66a**

A previous work has shown that another ubiquitous component of the Gram-negative bacterial cell wall, LPS, is detected in esophageal Gr66a+ bitter-sensing neurons via the TrpA1 cation channel [25]. To assess whether TrpA1 is implicated in the response of neurons to PGN, we performed *in vivo* calcium imaging in *dTrpA1* mutants. The fact that PGN-dependent activation of cells is conserved in TrpA1 mutants demonstrated that PGN and LPS are detected by different receptors and certainly trigger different pathways in bitter GRNs (Extended Data Fig. 3-1b). The non-GPCR gustatory receptor GR66a itself was also not involved in mediating the response to PGN. Altogether, these results suggest that PGRP-LC could be the dedicated receptor necessary for PGN detection and transduction in bitter-sensing neurons.

**Activation of the NF-κB/IMD pathway in bitter-sensing neurons modulate aversive behaviors**

The ability of PGN to activate calcium release in bitter GRNs prompted us to test whether PGN triggers aversive behaviors in flies. We tested this hypothesis using the FlyPAD device in a two-choice feeding assay (Fig.4a)[39]. When flies were given a choice between a sucrose only and a sucrose plus PGN solution, no obvious repulsive behavior towards PGN was detected (Fig.4b and Extended Data Fig. 4-1a, b). To further evaluate the phenotypical consequences associated with activation of the NF-κB/IMD pathway specifically in the Gr66a+ neurons, we overexpressed the upstream signaling receptor PGRP-LCa in these cells. This ectopic expression may hypersensitize the cells to PGN and has been shown to induce forced dimer receptor formation and hence to trigger downstream signaling in the absence of the ligand or with lower

amounts of it. In a two-choice feeding assay, flies in which PGRP-LCa was overexpressed in GR66a+ neurons, showed an increased repulsion towards solution containing PGN (Fig.4c). This behavior, which was not observed in control animals, was abolished by the simultaneous knockdown of the NF-κB/IMD downstream element *Fadd* (Fig. 4d). Thus, when sensitized following over-expression of the PGRP-LCa receptor, flies can discriminate, via the IMD pathway between a sucrose containing PGN solution and a sucrose only solution. Since lactic acid bacteria *Enterococci* are critical modulators to attract *Drosophila* to lay eggs on decaying food [40], we then tested whether IMD-dependent activation of bitter-sensing neurons would impact egg-laying site preference. Although we were unable to detect any bias of egg-laying toward PGN contaminated media (data not shown), we observed that PGRP-LCa overexpression in Gr66a+ neurons directly led to a decreased oviposition (Fig. 4e, f). This decreased egg-laying when PGRP-LCa is expressed in bitter-sensing gustatory neurons was confirmed using $Gr32a^{Gal4}$ as another bitter GRNs driver (Extended Data Fig. 4-1c). These results suggesting that NF-κB/IMD pathway activation in bitter GRNs reduces female egg-laying were further confirmed by showing that this effect could be suppressed by the simultaneous RNAi-mediated *Fadd* inactivation in Gr66a+ neurons (Fig. 4g). In contrast, simultaneous knockdown of the transcription factor *Relish* did not impact the egg-laying decrease, indicating that this transactivator is not required for this PGN-mediated behavioral response (Fig 4g). We previously showed that PGN-dependent NF-κB/IMD pathway activation in a subset of brain octopaminergic neurons was sufficient to reduce female egg-laying, a phenomenon reproduced with Kir2.1 overexpression in these neurons, suggesting the PGN-dependent inactivation of this octopaminergic neurons [20]. Importantly, inactivating the Gr66a+ cells via Kir2.1 expression did not phenocopy the egg-laying drop caused by inactivation of octopaminergic neurons, suggesting that PGRP-LCa overexpression triggered activation of Gr66a+ neurons instead (Extended Data Fig. 4-1d). Consistently, conditional Gr66a+ cells activation via TrpA1 overexpression, that leads to inward current flux of cations, decreased female egg-laying (Fig. 4h). Taken together, these data demonstrate that receptor and transducers of the NF-κB/IMD pathway (but not the downstream NF-κB transcription factor Relish) are expressed and functionally required in bitter-sensing-neurons to mediate a behavioral response towards PGN.

## Discussion

This study demonstrates that some neurons of the gustatory system detect the peptidoglycan, one of the main conserved and ubiquitous cell wall bacterial components. In bitter-sensing gustatory neurons, this detection is mainly mediated by the IMD pathway PGRP-LC receptor and

thus probably not by classical Gr proteins such as Gr66a. The PGN signal is transduced by the known cytosolic members of the IMD pathway such as Fadd and Dredd. Together with previous reports, these results confirm the key role played by the PGRP/IMD module in regulating many of the interactions between PGN and flies. This specific recognition step, which takes place at the cell membrane via PGRP-LC or within the cells via PGRP-LE, has been shown to control the production of anti-bacterial effectors by immune-competent cells, to alter the egg-laying rate of infected females and to allow the physiological adaptation of the flies to their infectious status [18, 19, 20, 28, 41, 42, 43]. Interestingly, while the initial MAMP/PRR recognition event is conserved among these processes, the downstream molecular mechanisms that transduce the signal are context-dependent. Whereas the PGN-dependent activation of an immune response in adipocytes, hemocytes or enterocytes and the inhibition of VUM III octopaminergic brain neurons rely on the nuclear NF-κB/Relish protein, the transcriptionally regulated effectors are likely to be different [10, 20]. The response of bitter-sensing-neurons to PGN depends on a non-canonical IMD pathway in which NF-κB/Relish is not required. Interestingly, PGRP-LC and some downstream IMD components are also required at the pre-synaptic terminal of *Drosophila* motoneurons for robust presynaptic homeostatic plasticity [44, 45]. The local modulation of the presynaptic vesicle release, which occurs in seconds following inhibition of postsynaptic glutamate receptors, required PGRP-LC, Tak1 but is also Relish-independent. These data and ours raise important questions regarding how the activation of the upstream elements of the IMD cascade is modifying neuronal activity, a topic for future studies. Previous biochemical studies have shown that IMD signaling is rapid, occurring in seconds, a time frame consistent with its role at the synapse and now in bitter-sensing neurons signal transduction[46]. Another possibility for the involvement of the IMD pathway in the bitter-sensing neurons would be that the expression of a yet to be identified PGN sensor requires the PGRP/IMD module for a permissive signal upon stimulation by environmental bacteria.

Our data show that flies can perceive PGN, a component of the bacteria cell wall, via bitter-sensing neurons. These findings are complementary to observations made for another cell wall component in Gram-negative bacteria, called LPS, which triggers feeding and oviposition avoidance in *Drosophila* through the activation of bitter-sensing neurons[25]. While LPS induced avoidance behavior is mediated through the canonical chemosensory cation channel TrpA1, we show that PGN induced activation of bitter-sensing neurons seems to be independent of it. It seems to be also independent of the classical Gr receptors but to depend on a dedicated PGN sensor used in other contexts. We demonstrate that the bitter response upon PGN stimulation is dependent on the IMD pathway that not only regulates a feeding aversion for PGN but also

modulate oviposition rate. This indicates that PGN detection by gustatory neurons and its relay by the IMD pathway is probably an informative environmental cue for flies. Our approach focusing on purified PGN allows us to directly link a molecule to the neurons and the molecules that perceive it. However, the behavior of flies in a natural environment most probably corresponds to a highly complex integration of multiple intricate signals perceived by different sensory systems of the animal. For instance, lactic acid, which is produced by some bacteria is also sensed by gustatory neurons[47]. In this respect, it remains difficult to appreciate to which concentrations of bacteria-derived products animal sensory system are exposed in their natural environment. Assays estimated the amount of LPS at the surface of fruits of around 1000µg/mL [25]. To our knowledge, no such studies were performed for PGN. It should also be mentioned that the amount of PGN released by bacteria is highly dependent on the species considered and the bacterial growth phase to cite only few parameters [48]. The ability of the PGN to serve as a ligand for its host receptor also depends on other cell wall component such as teichoic acid, but also on PGN degrading enzymes such as amidase or lysozymes that degrade it[49]. It is therefore complicated to speculate on what could be a physiological concentration of PGN for flies sensing its environment.

Thus, in nature, PGN is likely detected in combination with other tastants and odorants, which detected alone may lead to an array of conflicting behaviors but in combination will yield in one context-dependent behavioral output [25, 50]. Consequently, it may be hazardous to expect clear phenotypes, or to make sense of the observed ones for the ecology of the fly when testing a single molecule of the permanent environment of the animal while this molecule is not especially deleterious *per se*, but rather informative for the insect. The PGN is an interesting case as on one hand, an internal sensing of this molecule indicates an infection, the uncontrolled growth of a bacteria or a breach in a physical barrier. On the other hand, the perception of this same molecule in the environment might be a clue, among others, to suggest a heavily contaminated place.

## Figure legends

**Figure 1. An IMD pathway component is expressed in neurons located in the proboscis.** Detection of cells expressing pLB1$^{Gal4}$/UAS-mCD8-GFP (pLB1+). **a**. Schematic representing the fly head and the axonal projections of pLB1+ peripheral neurons (green). The proboscis is an appendix dedicated to the feeding process and hosting neurons dedicated to detection of tastants. The cell bodies of pLB1+ neurons are located in labellar sensilla exposed to the environment and project axons to the brain, specifically in the sub-esophageal zone (SEZ). **b**. In the brain of female flies, labellar pLB1+ neurons project in the SEZ with a reproducible pattern (n=25). The panel on the right is a magnification of the SEZ delineated by the white box. **c**. The projections seen in the SEZ arise from neurons whose cell bodies are located in the tip of the proboscis (Table 1, n=32), the labellum. The panel on the right is a magnification of the labellum delineated by the white box. **d**, **e**. Immunodetection in the brain (**d**) and detection in the proboscis (**e**) of cells expressing pLB1$^{Gal4}$/UAS-mCD8-GFP (pLB1+) as well as Gr66a-RFP (Gr66a+) (n=5 for brains and 6 for proboscices). **d**. Top left is a view of a large portion of the brain, the other panels are magnifications of the SEZ delineated by the white box. d, **e**. All the pLB1+ projections and neurons (arrowheads) are Gr66a+ while not all the Gr66a+ projections and cells (arrows) are pLB1+. Scale bar, 50 µm. n indicates the number of examined brains or proboscises. Stacks of images were analyzed. For the proboscises, sagittal views, anterior is on the right with dorsal part and maxillary palps sometimes visible at the bottom. See also Table 1, Table 2, extended Data Fig. 1-1 and Fig 1-2.

**Figure 2. Bitter gustatory receptor neurons respond to DAP-type peptidoglycan.** Real-time calcium imaging using the calcium indicator GCaMP6s to assess the *in vivo* neuronal activity in the sub-esophageal zone (SEZ) of labellar pLB1+ neurons (pLB1$^{Gal4}$/UAS-GCaMP6s) (**a, b**) or bitter gustatory receptor neurons (Gr66a$^{Gal4}$/UAS-GCaMP6s) (**c, d**). **a** and **c**. Representative images (top) and averaged fluorescence ± SEM time course of the GCaMP6s intensity variations (ΔF/F0%) (bottom). The addition of the chemical on the proboscis at a specific time is indicated by the arrow. **a**. The images illustrate the GCaMP6s intensity before and after the addition of either water as negative control (left panels), peptidoglycan (PGN 100 µg/mL; middle panels), caffeine or sucrose (right panels) on the proboscis. Scale bar, 20 µm. **c**. The images illustrate the GCaMP6s intensity before and after the addition of either water as negative control, *E.coli* K12 (OD600=0.5), peptidoglycan (PGN; 100 µg/mL), caffeine or sucrose (from left to right panel) on the proboscis. Scale bar, 20 µm. **b**. Averaged fluorescence

intensity of peaks (ΔF/F0) ± SD for control, PGN (different concentrations), caffeine or sucrose stimulated flies (n= 7-8). **d**. Averaged fluorescence intensity of peaks ± SD for control, *E.coli* K12(OD600=0.5), PGN (100 µg/mL), caffeine or sucrose stimulated flies (n=7-9). **e** and **f**. Averaged fluorescence intensity of peaks (ΔF/F0) ± SD for pLB1$^{Gal4}$/UAS-GCaMP6s (n=7-8) (**e**) or Gr66a$^{Gal4}$/UAS-GCaMP6s (n=7-8) (**f**) flies exposed to water, Lys-type PGN (100 µg/mL) or DAP-type PGN (100 µg/mL). n indicates the number of analyzed animals (single dots in graphs) for each condition. *** indicates $p < 0.0001$; non-parametric t-test, Mann-Whitney test.

**Figure 3. The PGN detection in pLB1+and Gr66a+ neurons requires upstream elements of the NF-κB/IMD pathway.**

**a**. Schematic of the canonical NF-κB/IMD pathway in *Drosophila*. **b-d**. Real-time calcium imaging using the calcium indicator GCaMP6s to assess the *in vivo* neuronal activity in the subesophageal zone (SEZ) of labellar pLB1+ neurons (pLB1$^{Gal4}$/UAS-GCaMP6s) (**b**) or bitter gustatory receptor neurons (Gr66a$^{Gal4}$/UAS-GCaMP6s) (**c**,**d**). **b**, **c**. Averaged fluorescence intensity of peaks (ΔF/F0) ± SD for pLB1$^{Gal4}$/UAS-GCaMP6s (n=8-9). (**b**) or Gr66a$^{Gal4}$/UAS-GCaMP6s (n=7-8) (**c**) flies in different mutant backgrounds and exposed to PGN (100 µg/mL). **d**. Averaged fluorescence intensity of peaks (ΔF/F0) ± SD for Gr66a$^{Gal4}$/UAS-GCaMP6s animals expressing RNAi targeting different elements of the NF-κB/IMD pathway and exposed to PGN (100 µg/mL) (n= 6-8). n indicates the number of analyzed animals (single dots in graphs) for each condition. *** indicates $p<0.0001$; non-parametric t-test, Mann-Whitney test. See also extended Data Fig. 3-1.

**Figure 4. Over-expression of the PGN receptor PGRP-LCa in bitter-sensing neurons modulates feeding preference towards peptidoglycan and oviposition behavior.**

**a**. Schematic of the two-choice feeding assay using the flyPAD device [39]. Individual flies are given the choice between a sucrose solution (5mM) and a sucrose solution (5mM) plus peptidoglycan (PGN) and tested for 1 hour. **b-d**. Feeding preference is expressed as a Preference Index (PI) based on the number of sips (see **Material and Methods**). **b**. Feeding preference of wild type (*Canton S*) flies exposed to two sucrose solutions (5mM), one of which containing PGN (different concentrations are tested and indicated in the X axis) (n=50-68). **c**. Feeding preference of flies overexpressing PGRP-LCa in bitter taste neurons (Gr66a$^{Gal4}$/UAS-PGRP-LCa) and controls exposed to two sucrose solutions (5mM), one of which containing PGN (100 µg/mL) (n= 61-73). **d**. Feeding preference of flies overexpressing simultaneously PGRP-LCa

and UAS Fadd RNAi in bitter taste neurons (Gr66a$^{Gal4}$/UAS-PGRP-LCa, UAS-Fadd RNAi) and control animals exposed to two sucrose solutions (5mM), one of which containing PGN (100 µg/mL) (n=49-52). **e**. Schematic of the oviposition assay. Individual flies are transferred in fresh tubes and allowed to lay eggs for 24 hours (24h). **f**. Eggs laid per 24h by flies overexpressing PGRP-LCa in bitter taste neurons (Gr66a$^{Gal4}$/UAS- PGRP-LCa) and control animals (n=80-92). **g**. Eggs laid per 24h by flies overexpressing simultaneously PGRP-LCa and Fadd RNAi or Relish RNAi in bitter-sensing gustatory neurons (Gr66$^{Gal4}$/UAS-PGRP-LCa, UAS-Fadd RNAi) and control animals (n=24-76). **h**. Eggs laid per 24h by flies overexpressing TrpA1 in bittersensing neurons (Gr66$^{Gal4}$/UAS-TrpA1) and control animals, at a permissive (23°C) and restrictive (29°C) temperature (n=18-20). **b-d**. shown are the average PI ± SD of at least three independent trials. *** indicates p<0.0001; ns indicates p > 0.05; non-parametric t-test, Mann-Whitney test. **f-h**. shown are the average numbers of eggs laid per fly per 24 h ± SD from at least two independent trials with at least 20 females per trial, genotype and condition used. *** indicates p<0.0001; ns indicates p > 0.05; non-parametric ANOVA, Dunn's multiple comparison test. n indicates number of analyzed animals (single dots in graphs) for each condition. See also extended Data Fig. 4-1.

## Extended data

**Figure 1-1. pLB2 and pLB3 expressions are not detected in the fly labellum.**

**a**. Schematic representation showing the PGRP-LB locus (adapted from FlyBase http://flybase.org/reports/FBgn0037906.html and from [18]. The exonic coding sequences are indicated in light purple, while the non-coding exonic sequence in dark purple. In green are represented the fragments used to generate the pLB1$^{Gal4}$, pLB2$^{Gal4}$ and pLB3$^{Gal4}$ constructs [18]. **b**. Detection in the labella of pLB1+ (pLB1$^{Gal4}$/UAS-mCD8-GFP; n=32), pLB2+ (pLB2$^{Gal4}$/UAS-mCD8-GFP; n=7) and pLB3+ (pLB3$^{Gal4}$/UAS-mCD8-GFP; n=3) cells (from left to right, respectively). Stacks of images were analyzed.

**Figure 1-2. pLB1+ neurons in the labellum are exclusively Gr66a+.**

**a**. Immunodetection in brain (top) and detection in the proboscis (bottom) of cells pLB1+ as well as Gr66a+ via genetic intersectional strategy (pLB1$^{Gal4}$, Gr66a$^{LexA}$/UAS*frt*STOP*frt*mCD8-GFP, LexAopFLP; n=5 brains and n=4 proboscices). Arrows point to pLB1+/Gr66a+ cellular bodies. **b**. Immunodetection in brain (top) and detection in the proboscis (bottom) of cells pLB1+ and Gr66a- (pLB1+/Gr66a-) via the expression of the Gal4 inhibitor Gal80 specifically

in Gr66a+ cells (pLB1$^{Gal4}$; UAS-mCD8-GFP/Gr66a$^{LexA}$, LexAopGal80; n=3 brains and n=4 proboscices). **c**. Immunodetection in the brain of cells pLB1+ as well as Gr32a+ via genetic intersectional strategy (pLB1$^{Gal4}$/Gr32a$^{LexA}$; UAS*frt*STOP*frt*mCD8GFP, LexAopFLP; n=3). **d**. Immunodetection in the brain of cells pLB1+ as well as Gr5a+ via genetic intersectional strategy (pLB1$^{Gal4}$, Gr5a$^{LexA}$/UAS*frt*STOP*frt*mCD8GFP, LexAopFLP; n=2). **e**. Detection in the proboscis of cells producing the endogenous PGRP-LB (PGRP-LB::GFP) as well as Gr66a-RFP (Gr66a+). All the PGRP-LB::GFP+ cells (arrowheads) are Gr66a+ while not all the Gr66a+ cells (arrows) are PGRP-LB::GFP+ (n=4). In **a**-**d**, the right panels are magnifications of the sub-esophageal zone delineated by the white box. All the images of the proboscis are sagittal views with anterior on the right and dorsal at the bottom. n indicates number of examined brains or proboscises. Scale bar, 50 μm.

**Figure 3-1. The NF-κB/IMD pathway is not required for bitter -sensing gustatory neurons response to caffeine and pLB1+ neurons response to PGN does not necessitate Gr66a or dTrpA1.**

Real-time calcium imaging using the calcium indicator GCaMP6s to assess the *in vivo* neuronal activity in the SEZ of pLB1+ (**a** and **b**) or Gr66a+ (**c** and **d**) neurons. **a**,**c**. Averaged fluorescence intensity of peaks (ΔF/F0) ± SD for pLB1$^{Gal4}$/UAS-GCaMP6s (n=6-7) (**a**) or Gr66a$^{Gal4}$/UAS-GCaMP6s (n=7-8) (**c**) flies in different mutant backgrounds exposed to caffeine (10mM). **b**. Averaged fluorescence intensity of peaks ± SD for pLB1$^{Gal4}$/UAS-GCaMP6s flies in different mutant backgrounds exposed to peptidoglycan (100 μg/mL) (n=6-8). **d**. Averaged fluorescence intensity of peaks ± SD for Gr66a$^{Gal4}$/UAS-GCaMP6s animals expressing RNAi against IMD pathway elements and exposed to caffeine (10mM) (n=7-8). n indicates the number of analyzed animals (single dots in graphs) for each condition. ns indicates $p > 0.05$; non-parametric t-test, Mann-Whitney test.

**Figure 4-1. While PGN is neither attractive nor aversive for wild type flies in two-choice feeding assay, IMD pathway activation in bitter-sensing neurons inhibits egg laying.**

**a**,**b**. Feeding preference of *yw* (n=82-99) (**a**) or *w* (n=50-63) (**b**) flies exposed to two sucrose solutions (5mM), one of which containing PGN (different concentrations are tested and indicated in the X axis). **c** Eggs laid per 24 hours (24h) by flies overexpressing PGRP-LCa in bitter-sensing gustatory neurons (Gr32a$^{Gal4}$/UAS- PGRP-LCa) and control animals (n=60). **d.** Eggs laid per 24 hours (24h) by flies overexpressing kir2.1 in bitter taste neurons (G66a$^{Gal4}$/UAS-kir2.1) and control animals (n=60). **a**,**b**. Shown are the average Preference Index (PI) ± SD of

at least 5 independent trials. *** indicates p<0.0001; ns indicates p > 0.05; non-parametric t-test, Mann-Whitney test. **c**,**d**. Shown are the average numbers of eggs laid per fly per 24 h ± SD from at least two independent trials with at least 20 females per trial, genotype and condition used. *** indicates p<0.0001; ns indicates p > 0.05; non-parametric ANOVA, Dunn's multiple comparison test. n indicates the number of analyzed animals (single dots in graphs) for each condition.

**Table 1. Number of GFP-positive neurons for labellum in pLB1$^{Gal4}$/UAS-mCD8-GFP flies.**

The amount of times (N) a precise quantity of pLB1+ neurons is detected (event) is shown over the total amount of proboscises observed. Only 1-week old female flies were analyzed.

**Table 2. Number of cells pLB1+ as well as Gr66a+ in labellum of pLB1$^{Gal4}$, UAS-mCD8-GFP/Gr66a-RFP 1-week old female flies.**

The amount of pLB1+ neurons, Gr66a+ neurons and co-stained cells are presented.

**Movie 1. pLB1+ neurons respond *in vivo* to PGN.**

Real-time calcium imaging using the calcium indicator GCaMP6s to assess the *in vivo* neuronal activity in the sub-esophageal zone of pLB1 neurons (pLB1$^{Gal4}$/UAS-GCaMP6s). Effect of peptidoglycan solution stimulation (100 µg/mL) on the proboscis. GFP signal was recorded every 500 ms and the PGN was added at 1 second after the beginning of the recording.

**Movie 2. pLB1+ neurons respond *in* vivo to caffeine.**

Real-time calcium imaging using the calcium indicator GCaMP6s to assess the *in vivo* neuronal activity in the sub-esophageal zone of pLB1 neurons (pLB1$^{Gal4}$/UAS-GcaMP6s). Effect of caffeine solution stimulation (10 mM) on the proboscis. GFP signal was recorded every 500 ms and the caffeine was added at 1 second after the beginning of the recording

**Movie 3. Gr66a+ neurons respond *in vivo* to PGN.**

Real-time calcium imaging using the calcium indicator GCaMP6s to assess the *in vivo* neuronal activity in the sub-esophageal zone of bitter-sensing neurons (Gr66a$^{Gal4}$/UAS-GCaMP6s). Effect of peptidoglycan solution stimulation (100 µg/mL). GFP signal was recorded every 500 ms and the PGN was added at 1 second after the beginning of the recording.

**Methods**

## Experimental designs

### Fly stocks

Detailled genotypes of all the flies used can be found in the **supplementary raw data** underlying the results.

All flies were maintained at 25°C on a standard cornmeal/agar medium on a 12 h:12 h light-dark cycle with a relative humidity of 70%.The strains used are the following: pLB1$^{Gal4}$ [18]; PGRP-LB::GFP [20]; w (BDSC:3605); yw ; Canton-S; Gr5a$^{LexA}$ [51, 52] (Gently provided by Dong Min Shin); Gr66a$^{LexA}$ ([53]; gently provided by K. Scott's Lab); Gr32a$^{LexA}$ [54] (gently provided by A. Dahanukar's lab); Gr32a$^{Gal4}$ (BDSC:57622); Gr66a$^{Gal4}$ ; Gr66a-RFP(X4) (BDSC:60691); UAS-TrpA1 (BDSC:26264,[55]); UAS-Kir2.1 (BDSC:6595); 40XUAS-mCD8-GFP (BDSC:32195); UAS-Fadd RNAi[56]; UAS-Imd RNAi (VDRC#101834) ; UAS-Dredd-RNAi (VDRC#104726); UAS-PGRP-LC RNAi (VDRC#101636); UAS-Relish RNAi (BDSC:28943); UAS*frt*STOP*frt* mCD8GFP (BDSC:30125); 8XLexAop2-FLP (BDSC:55819); UAS-GCaMP6s (BDSC:42746). UAS-PGRP-LCa [57]; PGRP-LC$^{E12}$ [58]; PGRP-LE$^{112}$ [59] ; PGRP-LB$^{ko}$ [60] ; Dredd$^{D55}$ [61]; TrpA1$^{1}$ [25].

### Tastants

For *in vivo* calcium imaging and flyPAD assays tastants were dissolved in autoclaved purified distilled water. All tastant solutions were freshly prepared and stored in aliquots at -20°C for a maximum duration of six months. Peptidoglycan was obtained from InvivoGen (PGN-EK Catalog # tlrl-pgnek, InvivoGen, USA), while sucrose (Roth, ref 4621.1) and caffeine (Sigma Aldrich, ref C0750) were obtained from Sigma-Aldrich (USA).

### *In vivo* calcium imaging

*In vivo* calcium imaging experiments were performed on 5-7 day-old starved mated females. Animals were raised on conventional media with males at 25°C ~~or 29°C for RNAi experiments~~. Flies were starved for 20-24 h in a tube containing a filter soaked in water prior any experiments. Flies of the appropriate genotype were anesthetized on ice for 1 h. Female flies were suspended by the neck on a plexiglass block (2 x 2 x 2.5 cm), with the proboscis facing the center of the block. Flies were immobilized using an insect pin (0.1 mm diameter) placed on the neck. The ends of the pin were fixed on the block with beeswax (Deiberit 502, Siladent, 209212). The head was then glued on the block with a drop of rosin (Gum rosin, Sigma-Aldrich -60895-, dissolved in ethanol at 70 %) to avoid any movements. The anterior part of the head was thus oriented towards the objective of the microscope. Flies were placed in a humidified box for 1 h to allow the rosin to harden without damaging the living tissues. A plastic coverslip

with a hole corresponding to the width of the space between the two eyes was placed on top of the head and fixed on the block with beeswax. The plastic coverslip was sealed on the cuticle with two-component silicon (Kwik-Sil, World Precision Instruments) leaving the proboscis exposed to the air. Ringer's saline (130 mM NaCl, 5 mM KCl, 2 mM $MgCl_2$, 2 mM $CaCl_2$, 36 mM saccharose, 5 mM HEPES, pH 7.3) was placed on the head[62]. The antenna area, air sacs, and the fat body were removed. The gut was cut without damaging the brain and taste nerves to allow visual access to the anterior ventral part of the sub-esophageal zone. The exposed brain was rinsed twice with Ringer's saline. GCaMP6s fluorescence was viewed with a Leica DM600B microscope under a 25x water objective. GCaMP6s was excited using a Lumencor diode light source at 482 nm ± 25. Emitted light was collected through a 505-530 nm band-pass filter. Images were collected every 500 ms using a Hamamatsu/HPF-ORCA Flash 4.0 camera and processed using Leica MM AF 2.2.9. Stimulation was performed by applying 140 µL of tastant solution diluted in water on the proboscis. For *E. coli* K12 stimulation, bacteria were grown in LB media overnight at 37°C, spined down 10 minutes at 3500g and the pellet suspended in water to obtain a final OD600 of 0.5. A minimum of 2 independent experiments with a total n for each condition ranging from 7 to 10 were performed. Each experiment consisted of a recording of 10 images before stimulation and 30 images after stimulation. Data were analyzed as previously described by using FIJI (https://fiji.sc/)[62]. In all experiments implicating $pLB1^{Gal4}$, this driver and the UAS-GCaMP6s transgenes are homozygous. In experiments using $Gr66a^{Gal4}$, the driver and the UAS-GCaMP6s transgenes are heterozygous.

**Immunostaining and imaging**

Immunostaining and imaging were performed as previously described[20]. Brains from adult females were dissected in Phosphate-buffered saline (PBS, Eurobio, ref CS0PBS0108) and fixed for 15 min in 4% paraformaldehyde (Electron Microscopy Sciences, Cat # 15714-S) at room temperature (RT). Afterward, brains were washed three times for 10 min in PBS-T (PBS + 0.3% Triton X-100) and blocked in 2,5% bovine serum albumin (BSA; Sigma-Aldrich) in PBS-T for 30 min. After saturation, samples were incubated with the primary antibody diluted in 0,5% BSA in PBS-T overnight at 4°C. The following day, brains were washed three times and incubated with the secondary antibody diluted in 0,5% BSA in PBS-T for 2 h at RT. Next, samples were washed for 10 min in PBS-T and mounted on slides using Vectashield (Vector Laboratories, Ca, USA) fluorescent mounting medium. In the case of proboscises, no immunostaining was performed. Proboscises of adult females were dissected in PBS, rinsed with PBS and directly mounted on slides using Vectashield fluorescent mounting medium. The tissues were visualized directly after.

For the immunostaining the primary antibodies used are the following: Chicken anti-GFP (Aves Labs Cat#GFP-1020, RRID:AB_10000240. Dilution 1:1000), rabbit anti-RFP (Rockland Cat#600-401-379, RRID:AB_2209751. Dilution 1:1000), mouse anti-NC82 (DSHB Cat#nc82,RRID:AB_2314866. Dilution 1:40). The secondary antibodies used are the following: Alexa Fluor 488 Donkey anti-Chicken IgY (IgG) (H+L) (Jackson ImmunoResearch Labs Cat#703-545-155, RRID:AB_2340375. Dilution 1:500), Alexa Fluor568 donkey anti-mouse IgG (H+L) (Thermo Fisher Scientific Cat#A10037, RRID:AB_2534013. Dilution 1:500), Alexa Fluor647 donkey anti-mouse IgG (H+L) (Jackson ImmunoResearch Labs Cat#715-605-151, RRID:AB_2340863. Dilution 1:500), Alexa Fluor 568 donkey anti-rabbit IgG (H+L) (Thermo Fisher Scientific Cat#A10042, RRID: AB2534017. Dilution 1:500).

Images were captured with either a Leica SP8 confocal microscope (in this case, tissues were scanned with 20X oil immersion objective) or an LSM 780 Zeiss confocal microscope (20x air objective was used). For the detection of endogenous PGRP-LB::GFP, images were captured with a Spinning Disk Ropper 2 Cam (20x or 40x air objective were used). Images were processed using Adobe Photoshop.

**Feeding assay**

5-7 day-old mated females were used. Animals were starved as a group for 20 h at 25°C prior to the assay in a tube containing a filter soaked in water. Previously, these females were raised with males on a conventional media at 25°C or 29°C for RNAi experiments. The assay could not last more than 1 h as the food is totally consumed after this period. Two-choice feeding assays were performed by using the flyPAD device[39] which records the cumulative number of sips. Each sip corresponds to a contact of flies' proboscis with the chosen food substrate. Individual flies were captured via aspiration (neither $CO^2$ nor ice used) and deposited in arenas containing two food substrates. The control substrate consisted in a 1% agarose 5mM sucrose solution, whereas the test substrate additionally contained peptidoglycan dissolved in water at the indicated concentrations. Each arena's well (2 per arena) was filled with 3.5 µL of food solution. Tests were run for 1 h at 25 °C under constant light in a behavioral room limiting the influence of external light and noise. Data were collected and analyzed by using Bonsai[63] and MATLAB, respectively (scripts provided by Pavel Itskov). Preference index was calculated as following: (number of sips in the test solution - number of sips in the control solution)/ total number of sips. Non eaters were excluded from the analysis.

**Oviposition assay**

Oviposition assays were performed as previously described[20]. 5 day-old mated females were used and raised on conventional media with males. Eclosed flies were raised at 25°C or 21°C, in case of experiments involving the thermosensitive transgene UAS-TrpA1 or 29°C for RNAi experiments. 5 day-old mated females were anesthetized on a $CO_2$ pad and singularly transferred in tubes containing a fresh (not older than 48h) conventional media with some dry yeast (Fermipan) on top of it right before the egg-lay period. Flies were let to lay eggs for 24 h at 25°c or 23°C in control conditions for experiments involving UAS-TrpA1 or 29°C for test conditions for experiments involving UAS-TrpA1 and RNAi experiments. After the egg-lay period, animals were discarded and eggs were counted using a binocular scope. At least two independent trials with at least 20 females per trial, genotype and condition were used.

**Statistical analysis**

Detailled statistical analyses and population sizes can be found in the **supplementary raw data** underlying the results.

***In vivo* calcium imaging**

D'Agostino & Pearson test to assay whether the values are distributed normally was applied. As not all the datasets were considered as normal, non-parametrical statistical analysis such as non-parametric unpaired Mann-Whitney two-tailed tests or non-parametric unpaired ANOVA, Kruskal-Wallis test, and Dunn's post-test were used for all the data presented.

**Feeding assay**

D'Agostino & Pearson test to assay whether the values are distributed normally was applied. As not all the datasets were considered as normal, non-parametrical statistical analysis such as non-parametric unpaired Mann-Whitney two-tailed tests or non-parametric unpaired ANOVA, Kruskal-Wallis test, and Dunn's post-test were used for all the data presented.

**Oviposition assay**

D'Agostino & Pearson test to assay whether the values are distributed normally was applied. As not all the datasets were considered as normal, non-parametrical statistical analysis and specifically the non-parametric unpaired ANOVA, Kruskal-Wallis test, and Dunn's post-test were used for all the data presented.

GraphPad Prism 8 software was used for statistical analyses. For *in vivo* calcium imaging and feeding assay analysis non-parametric unpaired Mann-Whitney two-tailed tests were

performed. In the case of oviposition assay, we used the non-parametric unpaired ANOVA, Kruskal-Wallis test, and Dunn's post-test.

1451
1452

**Acknowledgments**

We thank Emilie Avazeri and Annelise Viallat-Lieutaud for technical help. We thank members of the Royet's laboratory for their comments on the manuscript. This work was supported by (ANR-11-LABX-0054) (Investissements d'Avenir–Labex INFORM), ANR BACNEURODRO (ANR-17-CE16-0023-01) and ANR PEPTIMET (ANR-18-CE15-0018-02), Equipe Fondation pour la Recherche Médicale (EQU201903007783) and l'Institut Universitaire de France to J.R. Y.G. laboratory is supported by the "Centre National de la Recherche Scientifique", the "Université de Bourgogne Franche-Comté", the Conseil Régional Bourgogne Franche-Comte (PARI grant), the FEDER (European Funding for Regional Economical Development), and the European Council (ERC starting grant, GliSFCo-311403).

**Author contributions**

Genetic epistasis and imaging and behavioral assay were performed by A.M. and L.K. Calcium imaging was performed by G.M. Results were analyzed and interpreted by A.M., G.M., Y. G., L. K., and J. R. The original draft was written by J.R. Reviewing and editing were performed by all authors. Supervision: L.K., Y.G., and J.R. Funding acquisition: Y.G, and J.R.

**References**

1. Kavaliers, M., Ossenkopp, K.P. & Choleris, E. Pathogens, odors, and disgust in rodents. *Neurosci Biobehav Rev* **119**, 281-293 (2020).

2. Sullivan, K., Fairn, E. & Adamo, S.A. Sickness behaviour in the cricket Gryllus texensis: Comparison with animals across phyla. *Behav Processes* **128**, 134-143 (2016).

3. Mburu, D.M. *et al.* Relationship between virulence and repellency of entomopathogenic isolates of Metarhizium anisopliae and Beauveria bassiana to the termite Macrotermes michaelseni. *J Insect Physiol* **55**, 774-780 (2009).

4. Swanson, J.A. *et al.* Odorants that induce hygienic behavior in honeybees: identification of volatile compounds in chalkbrood-infected honeybee larvae. *J Chem Ecol* **35**, 1108-1116 (2009).

5. Hoffman, C. & Aballay, A. Role of neurons in the control of immune defense. *Curr Opin Immunol* **60**, 30-36 (2019).

6. Aranha, M.M. & Vasconcelos, M.L. Deciphering Drosophila female innate behaviors. *Curr Opin Neurobiol* **52**, 139-148 (2018).

7. Sayin, S., Boehm, A.C., Kobler, J.M., De Backer, J.F. & Grunwald Kadow, I.C. Internal State Dependent Odor Processing and Perception-The Role of Neuromodulation in the Fly Olfactory System. *Front Cell Neurosci* **12**, 11 (2018).

8. Masuzzo, A., Montanari, M., Kurz, L. & Royet, J. How Bacteria Impact Host Nervous System and Behaviors: Lessons from Flies and Worms. *Trends Neurosci* **43**, 998-1010 (2020).

9. Zhai, Z., Huang, X. & Yin, Y. Beyond immunity: The Imd pathway as a coordinator of host defense, organismal physiology and behavior. *Dev Comp Immunol* **83**, 51-59 (2018).

10. Buchon, N., Silverman, N. & Cherry, S. Immunity in Drosophila melanogaster--from microbial recognition to whole-organism physiology. *Nat Rev Immunol* **14**, 796-810 (2014).

11. Martino, M.E., Ma, D. & Leulier, F. Microbial influence on Drosophila biology. *Curr Opin Microbiol* **38**, 165-170 (2017).

12. You, H., Lee, W.J. & Lee, W.J. Homeostasis between gut-associated microorganisms and the immune system in Drosophila. *Curr Opin Immunol* **30**, 48-53 (2014).

13. Myllymaki, H., Valanne, S. & Ramet, M. The Drosophila imd signaling pathway. *J Immunol* **192**, 3455-3462 (2014).

14. Lindsay, S.A. & Wasserman, S.A. Conventional and non-conventional Drosophila Toll signaling. *Dev Comp Immunol* **42**, 16-24 (2014).

15. De Gregorio, E., Spellman, P.T., Tzou, P., Rubin, G.M. & Lemaitre, B. The Toll and Imd pathways are the major regulators of the immune response in Drosophila. *EMBO J* **21**, 2568-2579 (2002).

16. Royet, J., Gupta, D. & Dziarski, R. Peptidoglycan recognition proteins: modulators of the microbiome and inflammation. *Nat Rev Immunol* **11**, 837-851 (2011).

17. Kurata, S. Peptidoglycan recognition proteins in Drosophila immunity. *Dev Comp Immunol* **42**, 36-41 (2014).

18. Kurz, C.L., Charroux, B., Chaduli, D., Viallat-Lieutaud, A. & Royet, J. Peptidoglycan sensing by octopaminergic neurons modulates Drosophila oviposition. *Elife* **6** (2017).

19. Kobler, J.M., Rodriguez Jimenez, F.J., Petcu, I. & Grunwald Kadow, I.C. Immune Receptor Signaling and the Mushroom Body Mediate Post-ingestion Pathogen Avoidance. *Curr Biol* **30**, 4693-4709 e4693 (2020).

20. Masuzzo, A. *et al.* Peptidoglycan-dependent NF-kappaB activation in a small subset of brain octopaminergic neurons controls female oviposition. *Elife* **8** (2019).

21. Stensmyr, M.C. *et al.* A conserved dedicated olfactory circuit for detecting harmful microbes in Drosophila. *Cell* **151**, 1345-1357 (2012).

22. Min, S., Ai, M., Shin, S.A. & Suh, G.S. Dedicated olfactory neurons mediating attraction behavior to ammonia and amines in Drosophila. *Proc Natl Acad Sci U S A* **110**, E1321-1329 (2013).

23. Depetris-Chauvin, A., Galagovsky, D., Chevalier, C., Maniere, G. & Grosjean, Y. Olfactory detection of a bacterial short-chain fatty acid acts as an orexigenic signal in Drosophila melanogaster larvae. *Sci Rep* **7**, 14230 (2017).

24. Yanagawa, A., Neyen, C., Lemaitre, B. & Marion-Poll, F. The gram-negative sensing receptor PGRP-LC contributes to grooming induction in Drosophila. *PLoS One* **12**, e0185370 (2017).

25. Soldano, A. *et al.* Gustatory-mediated avoidance of bacterial lipopolysaccharides via TRPA1 activation in Drosophila. *Elife* **5** (2016).

26. Leulier, F. *et al.* The Drosophila immune system detects bacteria through specific peptidoglycan recognition. *Nat Immunol* **4**, 478-484 (2003).

27. Kaneko, T. *et al.* PGRP-LC and PGRP-LE have essential yet distinct functions in the drosophila immune response to monomeric DAP-type peptidoglycan. *Nat Immunol* **7**, 715-723 (2006).

28. Charroux, B. *et al.* Cytosolic and Secreted Peptidoglycan-Degrading Enzymes in Drosophila Respectively Control Local and Systemic Immune Responses to Microbiota. *Cell Host Microbe* **23**, 215-228 e214 (2018).

29. Lee, K.Z. & Ferrandon, D. Negative regulation of immune responses on the fly. *EMBO J* **30**, 988-990 (2011).

30. Chen, Y.D. & Dahanukar, A. Recent advances in the genetic basis of taste detection in Drosophila. *Cell Mol Life Sci* **77**, 1087-1101 (2020).

31. French, A. *et al.* Drosophila Bitter Taste(s). *Front Integr Neurosci* **9**, 58 (2015).

32. Montell, C. A taste of the Drosophila gustatory receptors. *Curr Opin Neurobiol* **19**, 345-353 (2009).

33. Weiss, L.A., Dahanukar, A., Kwon, J.Y., Banerjee, D. & Carlson, J.R. The molecular and cellular basis of bitter taste in Drosophila. *Neuron* **69**, 258-272 (2011).

34. Kwon, J.Y., Dahanukar, A., Weiss, L.A. & Carlson, J.R. A map of taste neuron projections in the Drosophila CNS. *J Biosci* **39**, 565-574 (2014).

35. Marella, S. *et al.* Imaging taste responses in the fly brain reveals a functional map of taste category and behavior. *Neuron* **49**, 285-295 (2006).

36. Thorne, N., Chromey, C., Bray, S. & Amrein, H. Taste perception and coding in Drosophila. *Curr Biol* **14**, 1065-1079 (2004).

37. Wang, Z., Singhvi, A., Kong, P. & Scott, K. Taste representations in the Drosophila brain. *Cell* **117**, 981-991 (2004).

38. Dunipace, L., Meister, S., McNealy, C. & Amrein, H. Spatially restricted expression of candidate taste receptors in the Drosophila gustatory system. *Curr Biol* **11**, 822-835 (2001).

39. Itskov, P.M. *et al.* Automated monitoring and quantitative analysis of feeding behaviour in Drosophila. *Nat Commun* **5**, 4560 (2014).

40. Liu, W. *et al.* Enterococci Mediate the Oviposition Preference of Drosophila melanogaster through Sucrose Catabolism. *Sci Rep* **7**, 13420 (2017).

41. Zhai, Z., Boquete, J.P. & Lemaitre, B. Cell-Specific Imd-NF-kappaB Responses Enable Simultaneous Antibacterial Immunity and Intestinal Epithelial Cell Shedding upon Bacterial Infection. *Immunity* **48**, 897-910 e897 (2018).

42. Guo, L., Karpac, J., Tran, S.L. & Jasper, H. PGRP-SC2 promotes gut immune homeostasis to limit commensal dysbiosis and extend lifespan. *Cell* **156**, 109-122 (2014).

43. Hedengren, M. *et al.* Relish, a central factor in the control of humoral but not cellular immunity in Drosophila. *Mol Cell* **4**, 827-837 (1999).

44. Harris, N. *et al.* The Innate Immune Receptor PGRP-LC Controls Presynaptic Homeostatic Plasticity. *Neuron* **88**, 1157-1164 (2015).

45. Harris, N., Fetter, R.D., Brasier, D.J., Tong, A. & Davis, G.W. Molecular Interface of Neuronal Innate Immunity, Synaptic Vesicle Stabilization, and Presynaptic Homeostatic Plasticity. *Neuron* **100**, 1163-1179 e1164 (2018).

46. Stoven, S., Ando, I., Kadalayil, L., Engstrom, Y. & Hultmark, D. Activation of the Drosophila NF-kappaB factor Relish by rapid endoproteolytic cleavage. *EMBO Rep* **1**, 347-352 (2000).

47. Stanley, M., Ghosh, B., Weiss, Z.F., Christiaanse, J. & Gordon, M.D. Mechanisms of lactic acid gustatory attraction in Drosophila. *Curr Biol* **31**, 3525-3537 e3526 (2021).

48. Travassos, L.H. *et al.* Toll-like receptor 2-dependent bacterial sensing does not occur via peptidoglycan recognition. *EMBO Rep* **5**, 1000-1006 (2004).

49. Vaz, F. *et al.* Accessibility to Peptidoglycan Is Important for the Recognition of Gram-Positive Bacteria in Drosophila. *Cell Rep* **27**, 2480-2492 e2486 (2019).

50. Lopez-Requena, A. *et al.* Roles of Neuronal TRP Channels in Neuroimmune Interactions. In: nd & Emir, T.L.R. (eds). *Neurobiology of TRP Channels*: Boca Raton (FL), 2017, pp 277-294.

51. Kim, H. *et al.* Drosophila Gr64e mediates fatty acid sensing via the phospholipase C pathway. *PLoS Genet* **14**, e1007229 (2018).

52. Mishra, D. *et al.* The molecular basis of sugar sensing in Drosophila larvae. *Curr Biol* **23**, 1466-1471 (2013).

53. Thistle, R., Cameron, P., Ghorayshi, A., Dennison, L. & Scott, K. Contact chemoreceptors mediate male-male repulsion and male-female attraction during Drosophila courtship. *Cell* **149**, 1140-1151 (2012).

54. Fan, P. *et al.* Genetic and neural mechanisms that inhibit Drosophila from mating with other species. *Cell* **154**, 89-102 (2013).

55. Hardie, R.C. *et al.* Calcium influx via TRP channels is required to maintain PIP2 levels in Drosophila photoreceptors. *Neuron* **30**, 149-159 (2001).

56. Khush, R.S., Cornwell, W.D., Uram, J.N. & Lemaitre, B. A ubiquitin-proteasome pathway represses the Drosophila immune deficiency signaling cascade. *Curr Biol* **12**, 1728-1737 (2002).

57. Maillet, F., Bischoff, V., Vignal, C., Hoffmann, J. & Royet, J. The Drosophila peptidoglycan recognition protein PGRP-LF blocks PGRP-LC and IMD/JNK pathway activation. *Cell Host Microbe* **3**, 293-303 (2008).

58. Gottar, M. *et al.* The Drosophila immune response against Gram-negative bacteria is mediated by a peptidoglycan recognition protein. *Nature* **416**, 640-644 (2002).

59. Takehana, A. *et al.* Peptidoglycan recognition protein (PGRP)-LE and PGRP-LC act synergistically in Drosophila immunity. *EMBO J* **23**, 4690-4700 (2004).

60. Paredes, J.C., Welchman, D.P., Poidevin, M. & Lemaitre, B. Negative regulation by amidase PGRPs shapes the Drosophila antibacterial response and protects the fly from innocuous infection. *Immunity* **35**, 770-779 (2011).

61. Leulier, F., Rodriguez, A., Khush, R.S., Abrams, J.M. & Lemaitre, B. The Drosophila caspase Dredd is required to resist gram-negative bacterial infection. *EMBO Rep* **1**, 353-358 (2000).

62. Silbering, A.F., Bell, R., Galizia, C.G. & Benton, R. Calcium imaging of odor-evoked responses in the Drosophila antennal lobe. *J Vis Exp* (2012).

63. Lopes, G. *et al.* Bonsai: an event-based framework for processing and controlling data streams. *Front Neuroinform* **9**, 7 (2015).

1687

# Figure 1

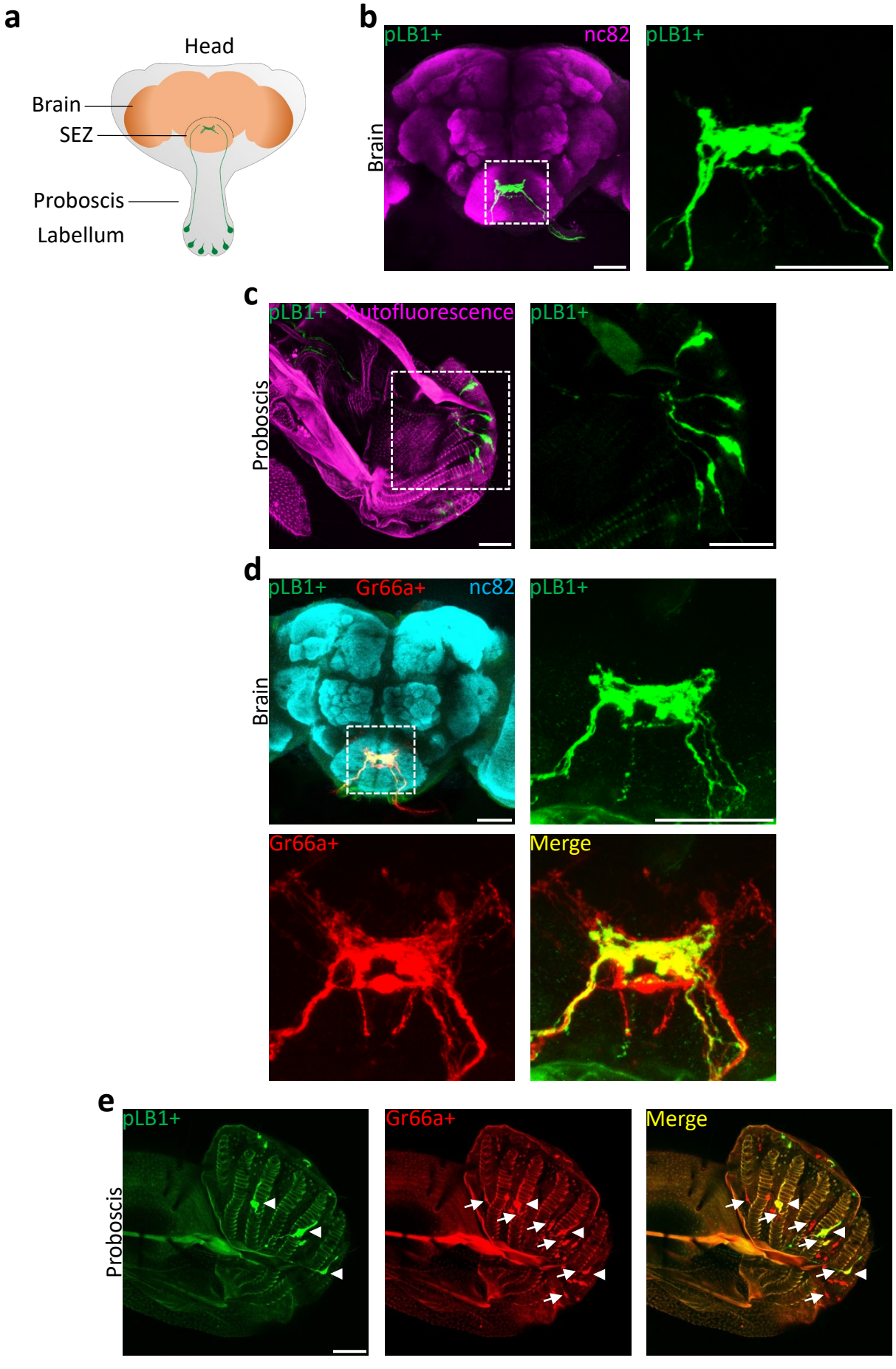
a
Head
Brain
SEZ
Proboscis
Labellum
b
pLB1+
nc82
Brain
pLB1+
c
pLB1+
Autofluorescence
Proboscis
pLB1+
d
pLB1+
Gr66a+
nc82
Brain
pLB1+
Gr66a+
Merge
e
pLB1+
Proboscis
Gr66a+
Merge

# Figure 2

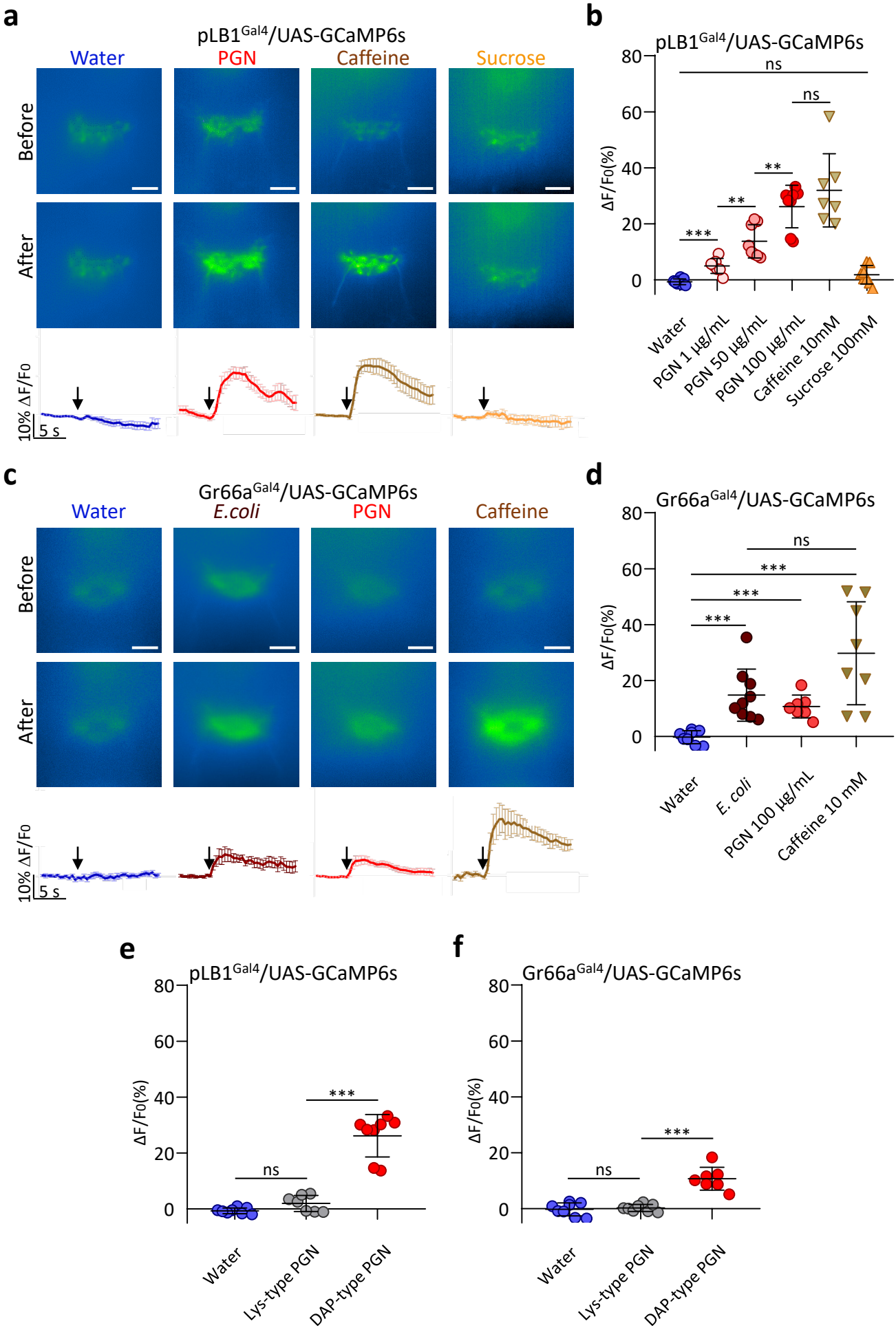
a
pLB1Gal4/UAS-GCaMP6s
Water
PGN
Caffeine
Sucrose
Before
After
10% ΔF/F0
5 s
b
pLB1Gal4/UAS-GCaMP6s
ΔF/F0(%)
ns
ns
**
**
***
Water
PGN 1 µg/mL
PGN 50 µg/mL
PGN 100 µg/mL
Caffeine 10mM
Sucrose 100mM
c
Gr66aGal4/UAS-GCaMP6s
Water
E.coli
PGN
Caffeine
Before
After
10% ΔF/F0
5 s
d
Gr66aGal4/UAS-GCaMP6s
ΔF/F0(%)
ns
***
***
***
Water
E. coli
PGN 100 µg/mL
Caffeine 10 mM
e
pLB1Gal4/UAS-GCaMP6s
ΔF/F0(%)
ns
***
Water
Lys-type PGN
DAP-type PGN
f
Gr66aGal4/UAS-GCaMP6s
ΔF/F0(%)
ns
***
Water
Lys-type PGN
DAP-type PGN

# Figure 3

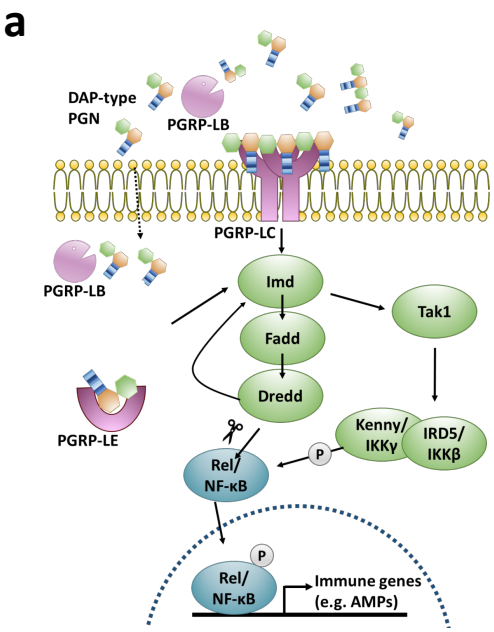
a
DAP-type PGN
PGRP-LB
PGRP-LC
PGRP-LB
Imd
Fadd
Dredd
Tak1
PGRP-LE
Kenny/ IKKγ
IRD5/ IKKβ
P
Rel/ NF-κB
P
Rel/ NF-κB
Immune genes (e.g. AMPs)

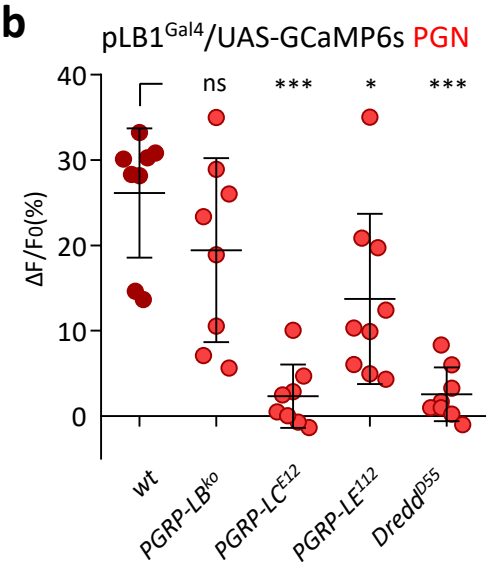
b
pLB1Gal4/UAS-GCaMP6s PGN
ΔF/F0(%)
40
30
20
10
0
ns
***
*
***
wt
PGRP-LBko
PGRP-LCE12
PGRP-LE112
DreddD55

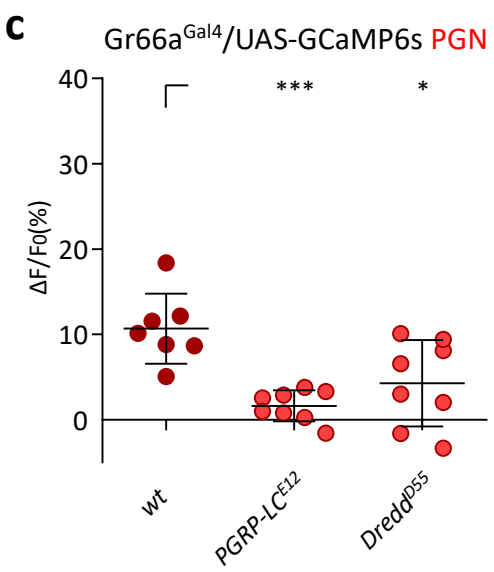
c
Gr66aGal4/UAS-GCaMP6s PGN
ΔF/F0(%)
40
30
20
10
0
***
*
wt
PGRP-LCE12
DreddD55

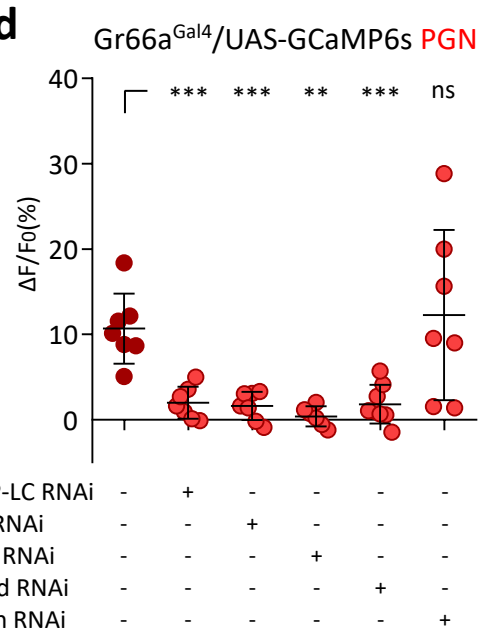
d
Gr66aGal4/UAS-GCaMP6s PGN
ΔF/F0(%)
40
30
20
10
0
***
***
**
***
ns
UAS-PGRP-LC RNAi - + - - - -
UAS-Imd RNAi - - + - - -
UAS-Fadd RNAi - - - + - -
UAS-Dredd RNAi - - - - + -
UAS-Relish RNAi - - - - - +

# Figure 4

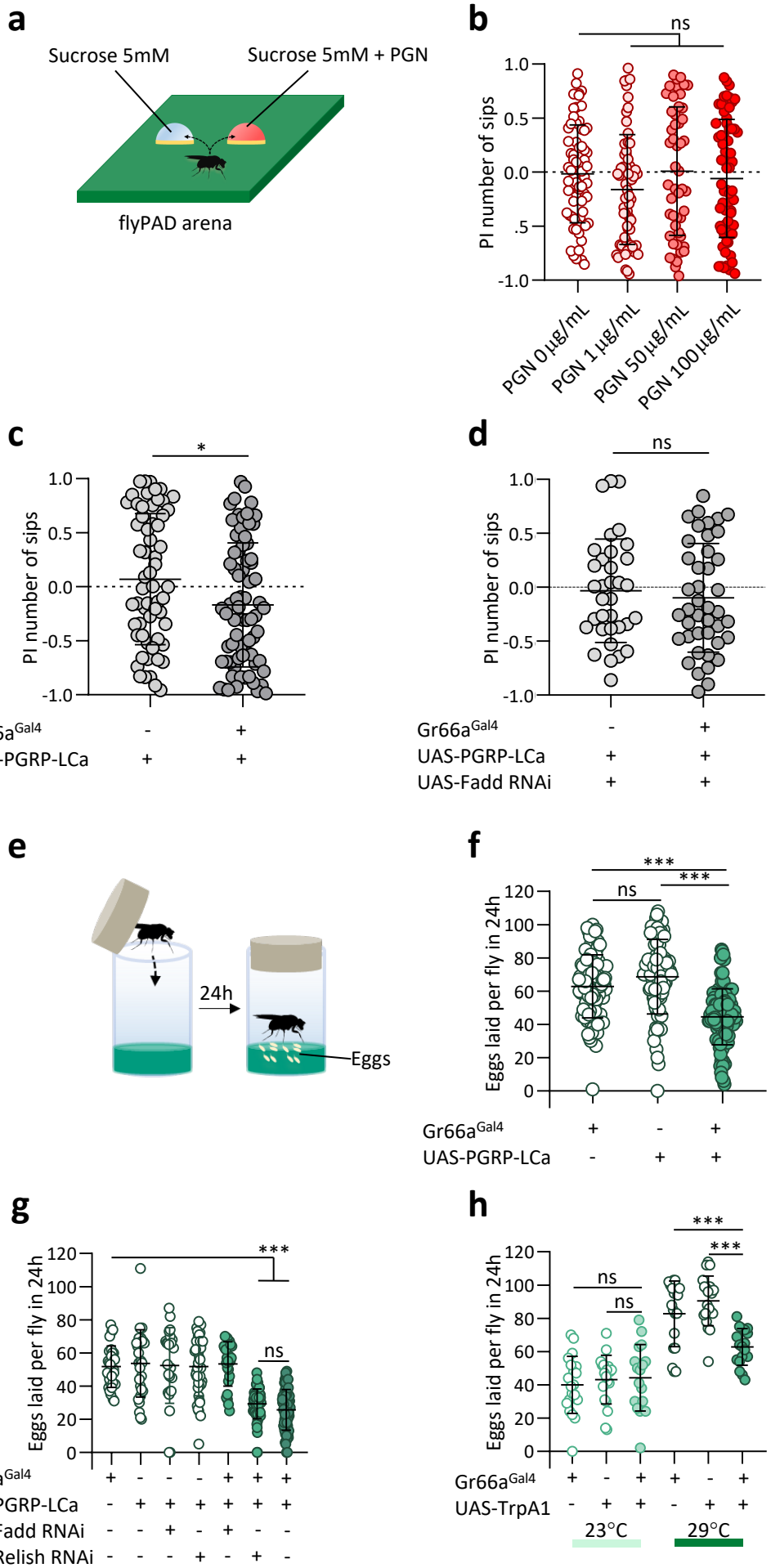
a
Sucrose 5mM
Sucrose 5mM + PGN
flyPAD arena
b
ns
PI number of sips
1.0
0.5
0.0
.5
-1.0
PGN 0 µg/mL
PGN 1 µg/mL
PGN 50 µg/mL
PGN 100 µg/mL
c
*
PI number of sips
1.0
0.5
0.0
-0.5
-1.0
Gr66a^Gal4 - +
UAS-PGRP-LCa + +
d
ns
PI number of sips
1.0
0.5
0.0
-0.5
-1.0
Gr66a^Gal4 - +
UAS-PGRP-LCa + +
UAS-Fadd RNAi + +
e
24h
Eggs
f
***
***
ns
Eggs laid per fly in 24h
120
100
80
60
40
20
0
Gr66a^Gal4 + - +
UAS-PGRP-LCa - + +
g
***
ns
Eggs laid per fly in 24h
120
100
80
60
40
20
0
Gr66a^Gal4 + - - - + + +
UAS-PGRP-LCa - + + + + + +
UAS-Fadd RNAi - - + - + - -
UAS-Relish RNAi - - - + - + -
h
***
***
ns
ns
Eggs laid per fly in 24h
120
100
80
60
40
20
0
Gr66a^Gal4 + - + + - +
UAS-TrpA1 - + + - + +
23°C
29°C

# Table 1

| Number of observed pLB1+ neurons (event) | N events/ Total number of proboscis |
|---|---|
| 3 | 5/32 |
| 4 | 6/32 |
| 5 | 11/32 |
| 6 | 6/32 |
| 7 | 3/32 |
| 8 | 1/32 |

# Table 2

| Number of observed pLB1+ neurons | Number of observed Gr66a+ neurons | Number of observed pLB1+/Gr66a+ neurons |
|---|---|---|
| 4 | 19 | 4 |
| 3 | 20 | 3 |
| 3 | 19 | 3 |
| 3 | 17 | 3 |
| 3 | 20 | 3 |
| 4 | 15 | 4 |